

Electronic Supplementary Information

Selective Separation and Preconcentration of Th(IV) Using Organo-Functionalized, Hierarchically Porous Silica Monoliths

Yimu Hu,^{a,b,c} Simon Giret,^{a,b,c} Rafael Meinusch,^d Jongho Han,^{e,f} Frédéric-Georges,^{*a,c,g} Freddy Kleitz,^{*h} and Dominic Larivière,^{*a,c}

^a Department of Chemistry, Université Laval, Québec, G1V 0A6, QC, Canada

^b Centre de Recherche sur les Matériaux Avancés (CERMA), Université Laval, Québec, G1V 0A6, QC, Canada

^c Centre en Catalyse et Chimie Verte (C3V), Université Laval, Québec, G1V 0A6, QC, Canada

^d Institute of Physical Chemistry, Justus-Liebig-University Giessen, 35392 Giessen, Germany

^e Department of Chemistry, Korea Advanced Institute of Science and Technology (KAIST), Daejeon 305-701, Republic of Korea

^f Center for Nanomaterials and Chemical Reactions, Institute for Basic Science, Daejeon 305-701, Republic of Korea

^g Canada Research Chair in Green Catalysis and Metal-Free Processes

^h Department of Inorganic Chemistry – Functional Materials, Faculty of Chemistry, University of Vienna, 1090 Vienna, Austria

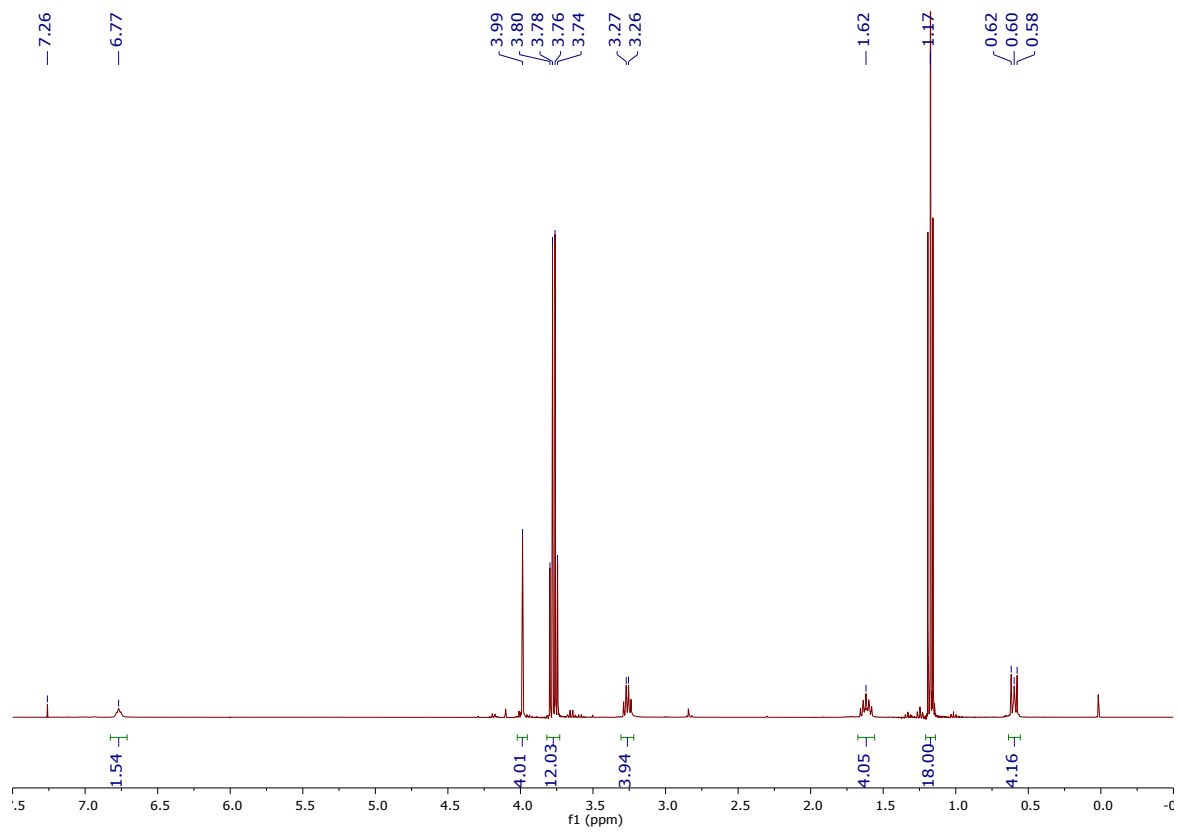
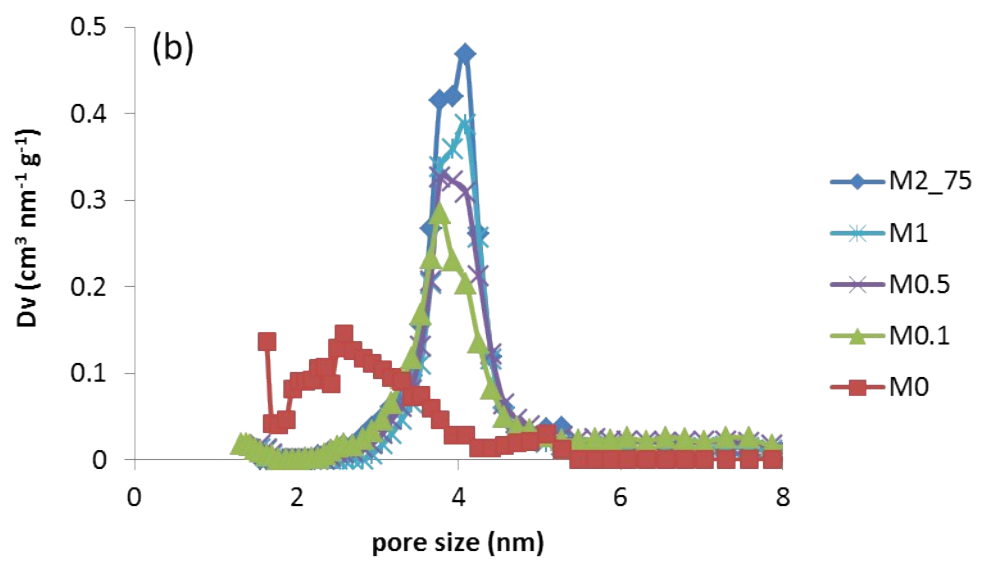
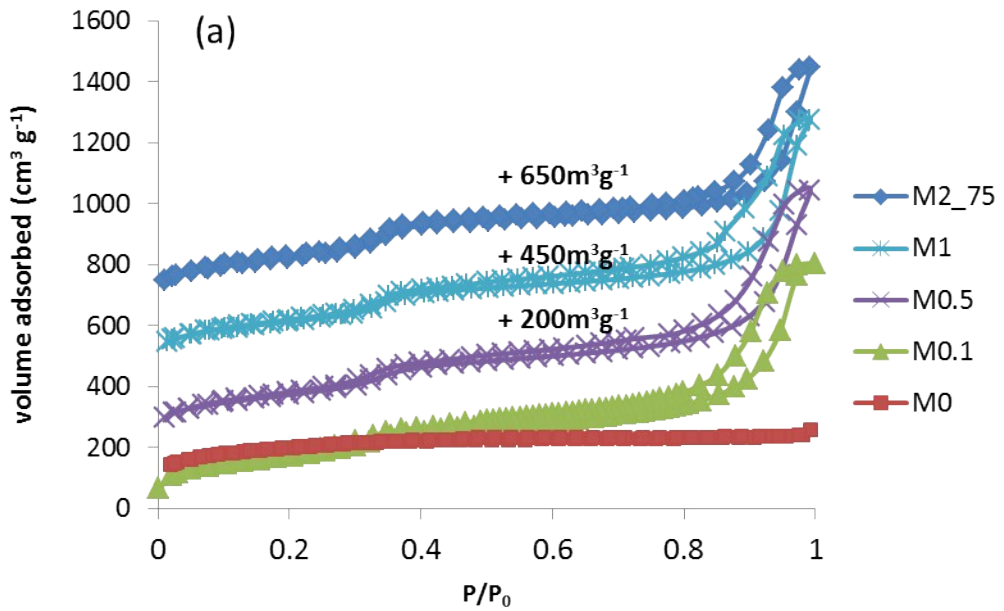


Figure S1. ¹H NMR of DGA-APTS (*chloroform-d*, 400 MHz).



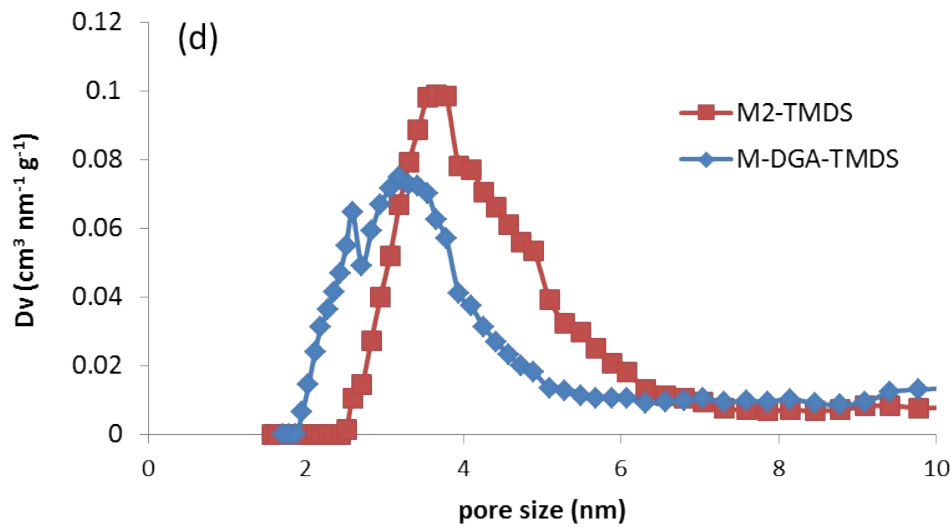
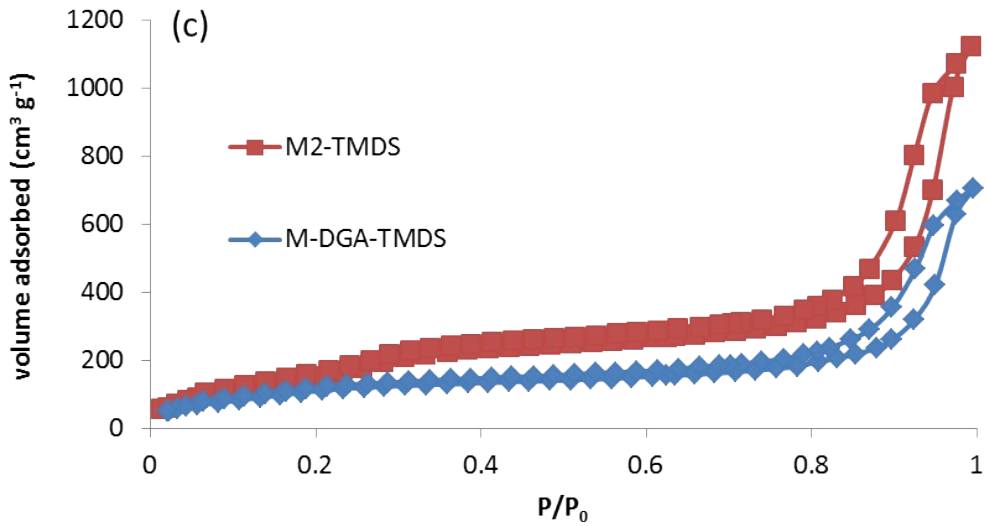
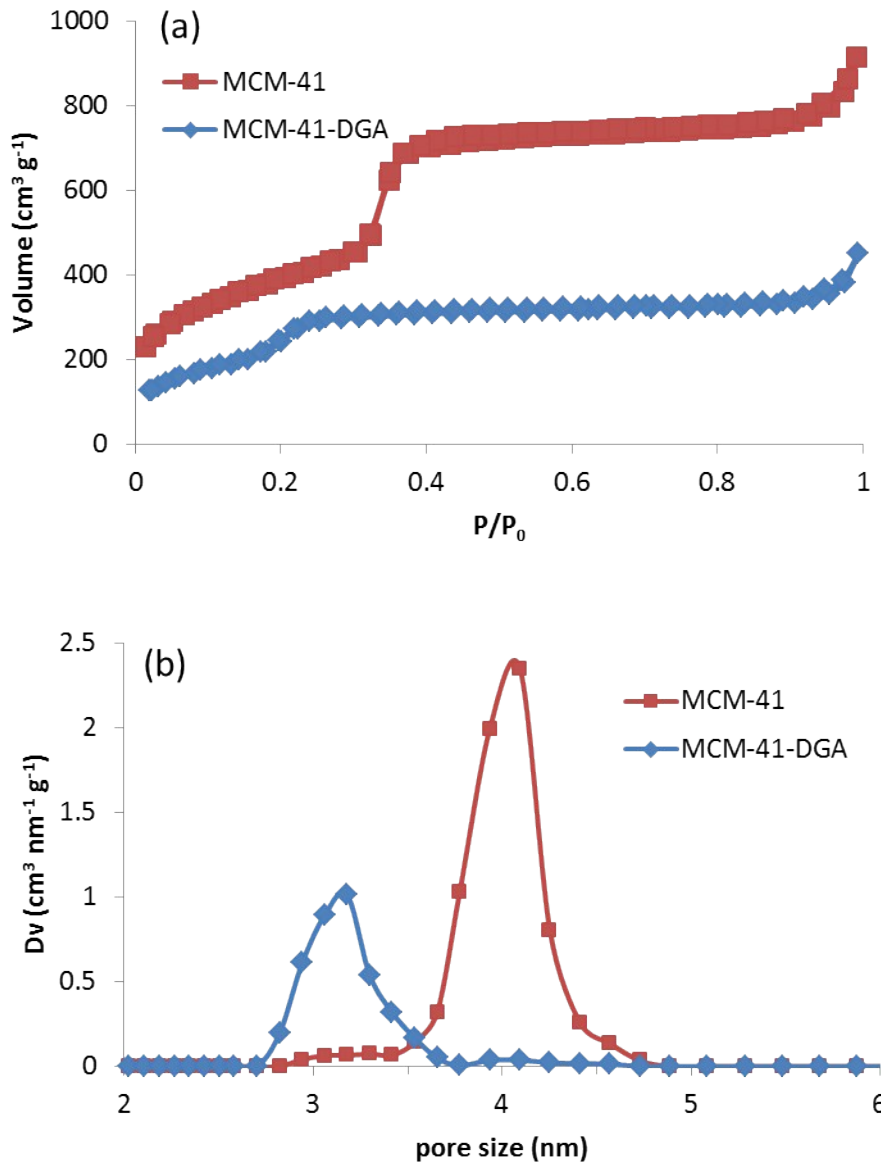


Figure S2. N₂ adsorption-desorption isotherms at -196 °C and the corresponding pore size distributions (PSD) calculated from the adsorption branch using the NLDFT method for the synthesized materials M2_75, M1, M0.5, M0.1, and M0 (a, b) and the passivated monoliths M2-TMDS and M-DGA-TMDS (c, d).



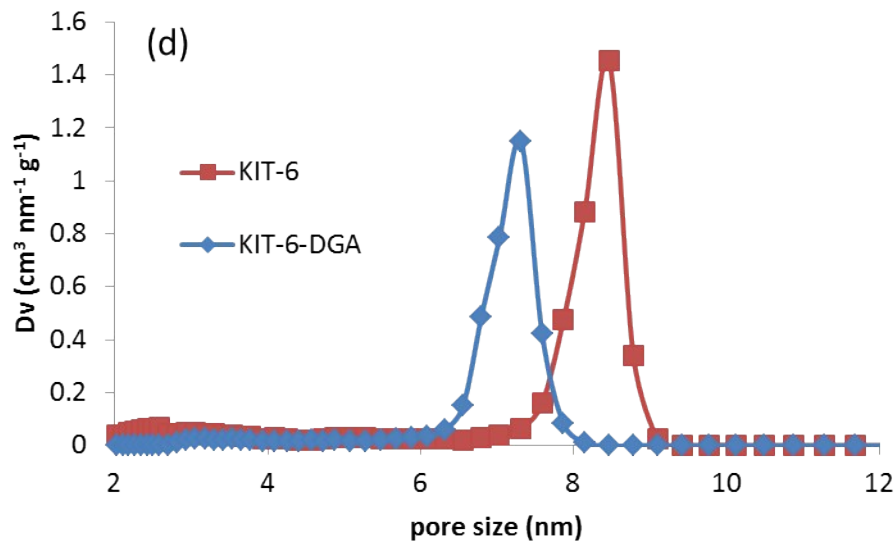
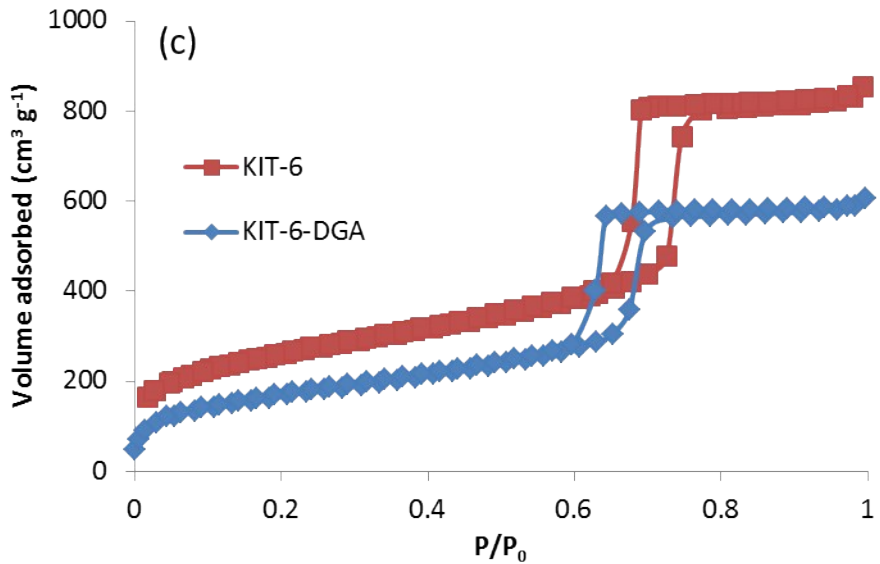
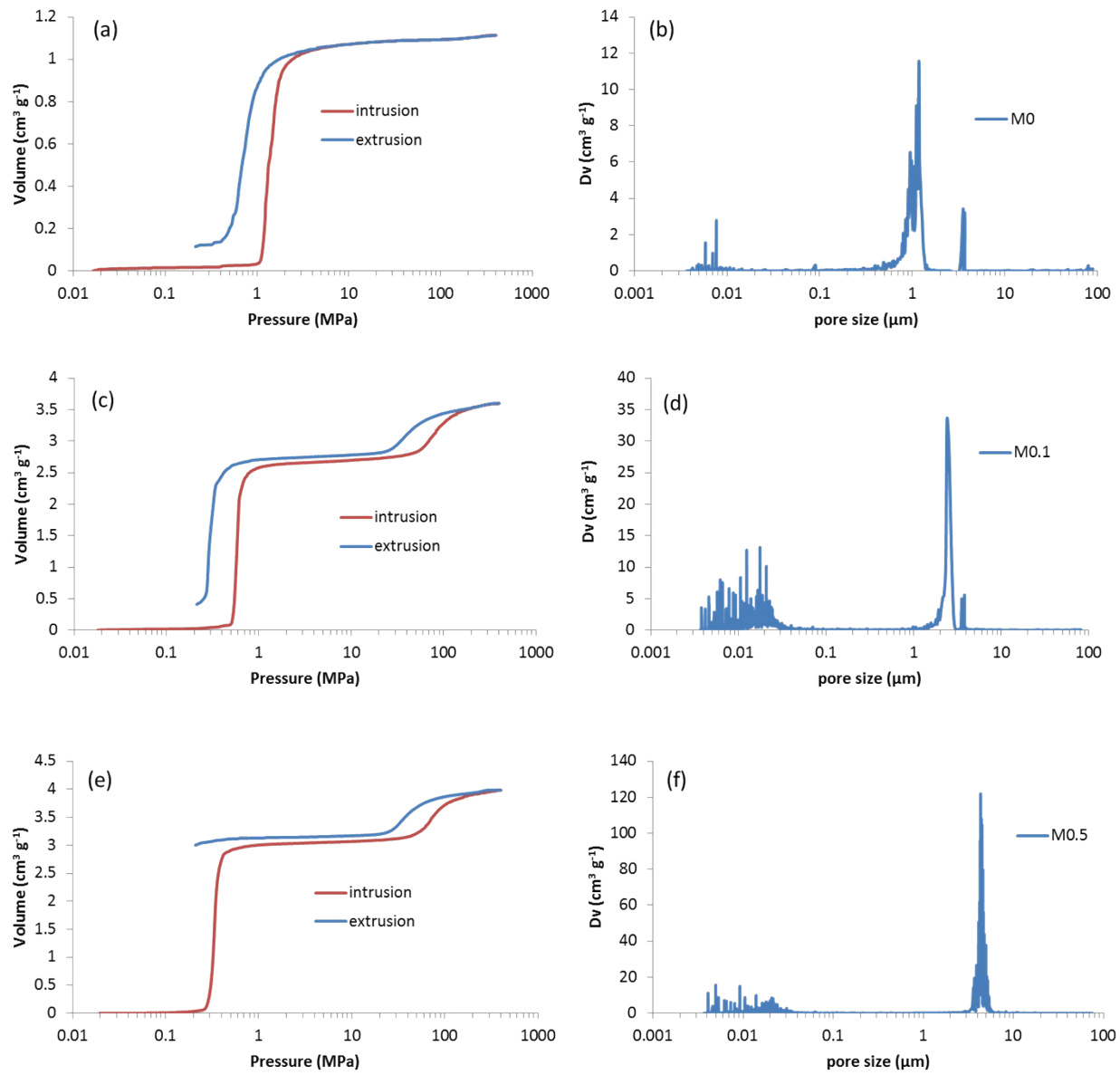


Figure S3. N₂ adsorption-desorption isotherms at -196 °C and the corresponding pore size distributions calculated from the equilibrium model (desorption branch) using the NLDFT method for the mesoporous materials MCM-41 and MCM-41-DGA (a, b), and KIT-6 and KIT-6-DGA (c, d).



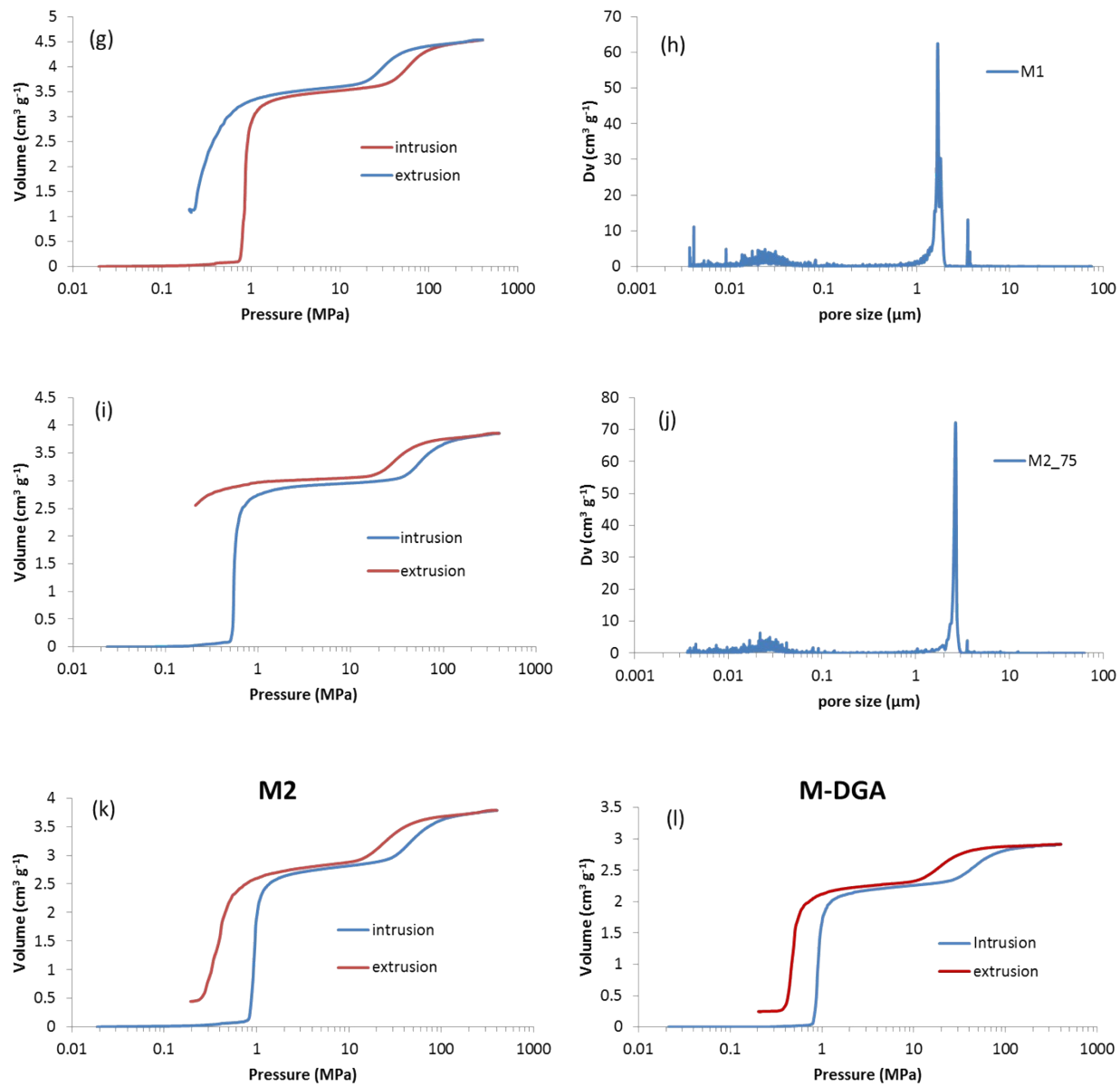


Figure S4. (From top to bottom) Mercury porosimetry intrusion/extrusion curves and corresponding pore size distributions of M0 (a, b), M0.1 (c, d), M0.5 (e, f), M1 (g, h), M2_75 (i, j). The pore size distributions for M2 (k) and M-DGA (l) can be found in the Figure 2 (c) and (d).

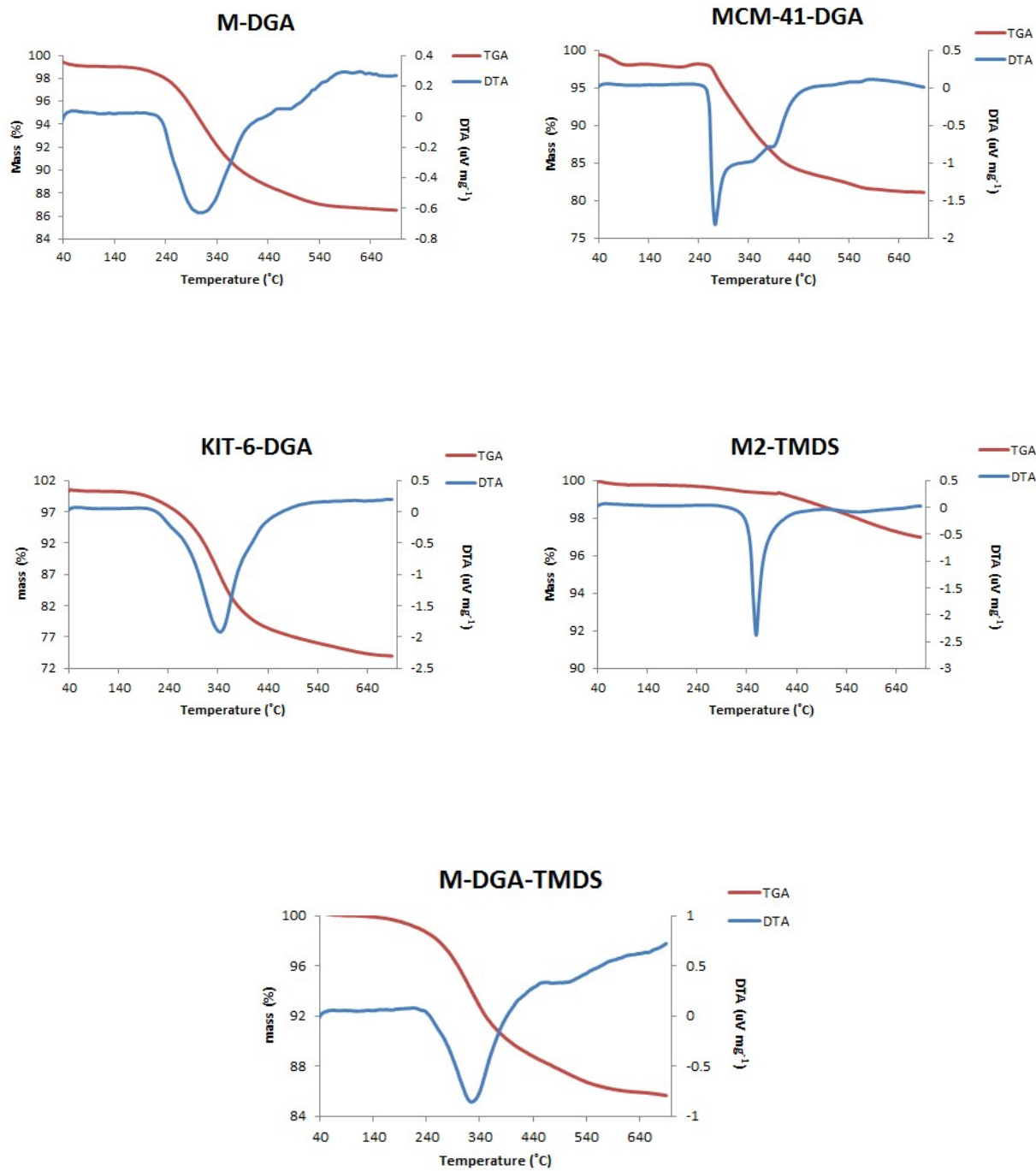


Figure S5. The thermogravimetric analysis (TGA, red) and differential thermal analysis (DTA, blue) curves of the functionalized materials (M-DGA, MCM-41-DGA, KIT-6-DGA) and the monoliths after surface passivation (M2-TMDS and M-DGA-TMDS).

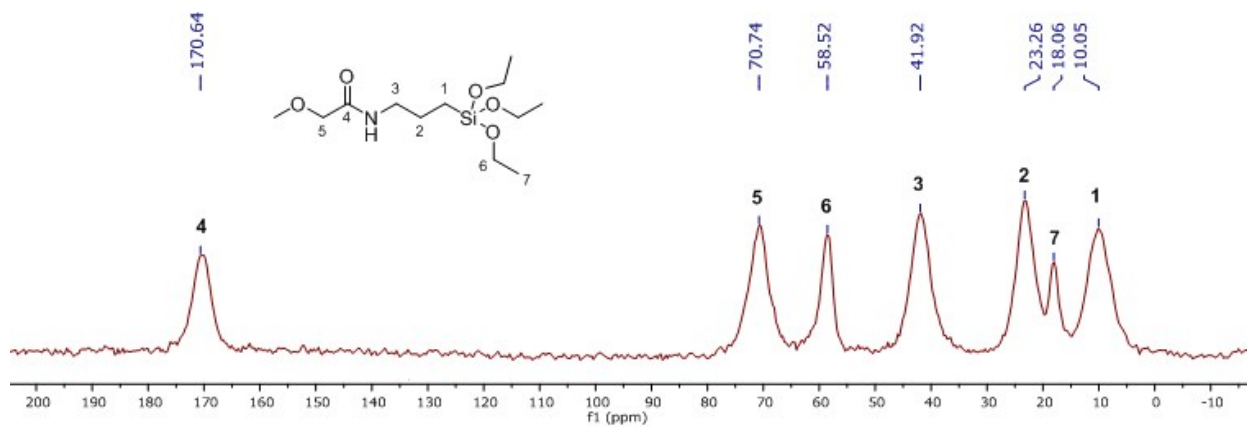


Figure S6. Solid state ^{13}C CP/MAS NMR spectrum for the DGA-functionalized monolith (M-DGA).

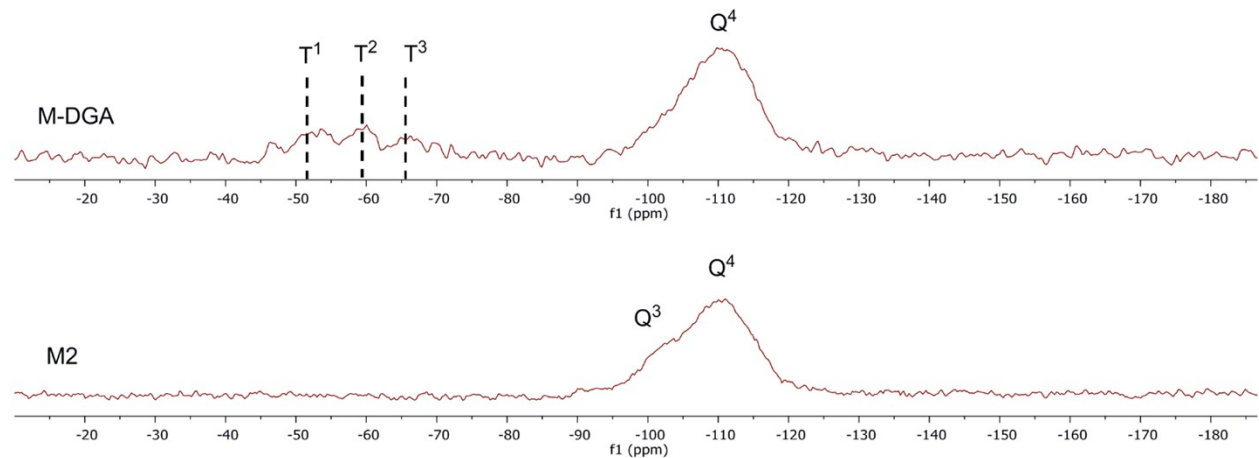


Figure S7. Solid state ^{29}Si MAS NMR spectra for the pristine monolith M2 and DGA-functionalized monolith M-DGA.

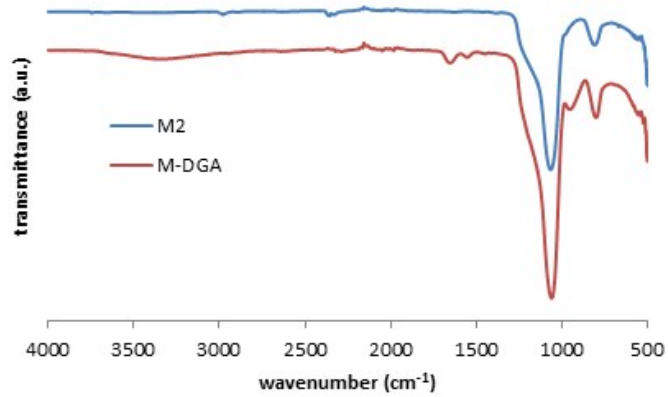


Figure S8. FTIR spectra of the pristine silica monolith M2 and the functionalized M-DGA. The spectra are normalized to the intensity of the SiO₂ band at 1041 cm⁻¹.

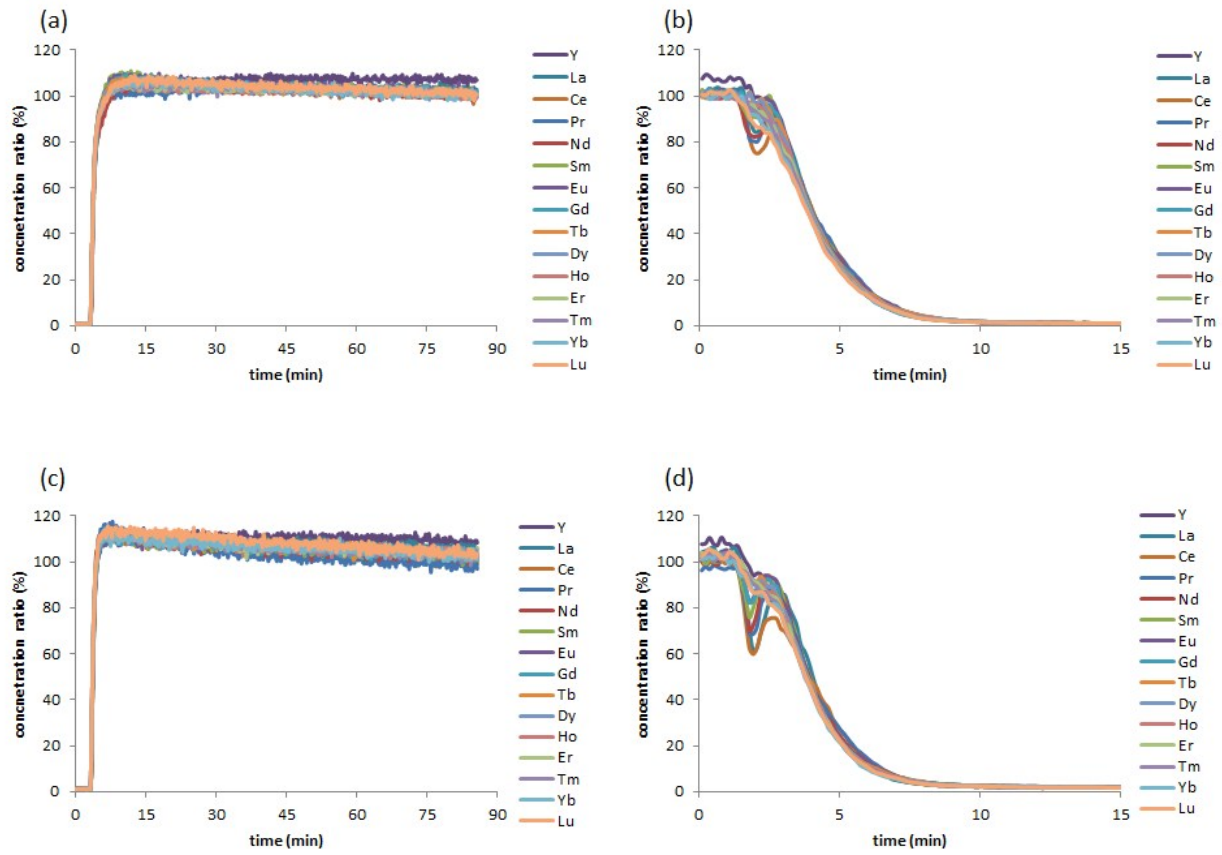


Figure S9. Extraction chromatograms of rare earth elements (REEs, from Y to Lu) with M-DGA (a) and M2 (c), and the corresponding recovery chromatograms of using 0.05 M ammonium oxalate (b and d). The initial feed solution contains REEs, Al, Fe, Th, and U (concentration of 300 $\mu\text{g L}^{-1}$, pH 3.0).

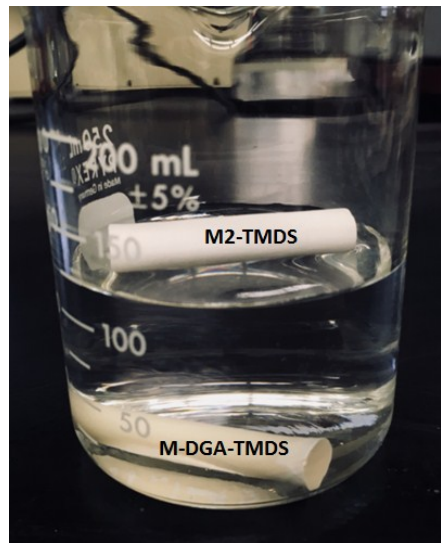


Figure S10. Photograph of M2-TMDS and M-DGA-TMDS in water after surface passivation. M2-TMDS floats in water due to the strong surface hydrophobicity, while M-DGA-TMDS, which is partly passivated, falls down to the bottom.

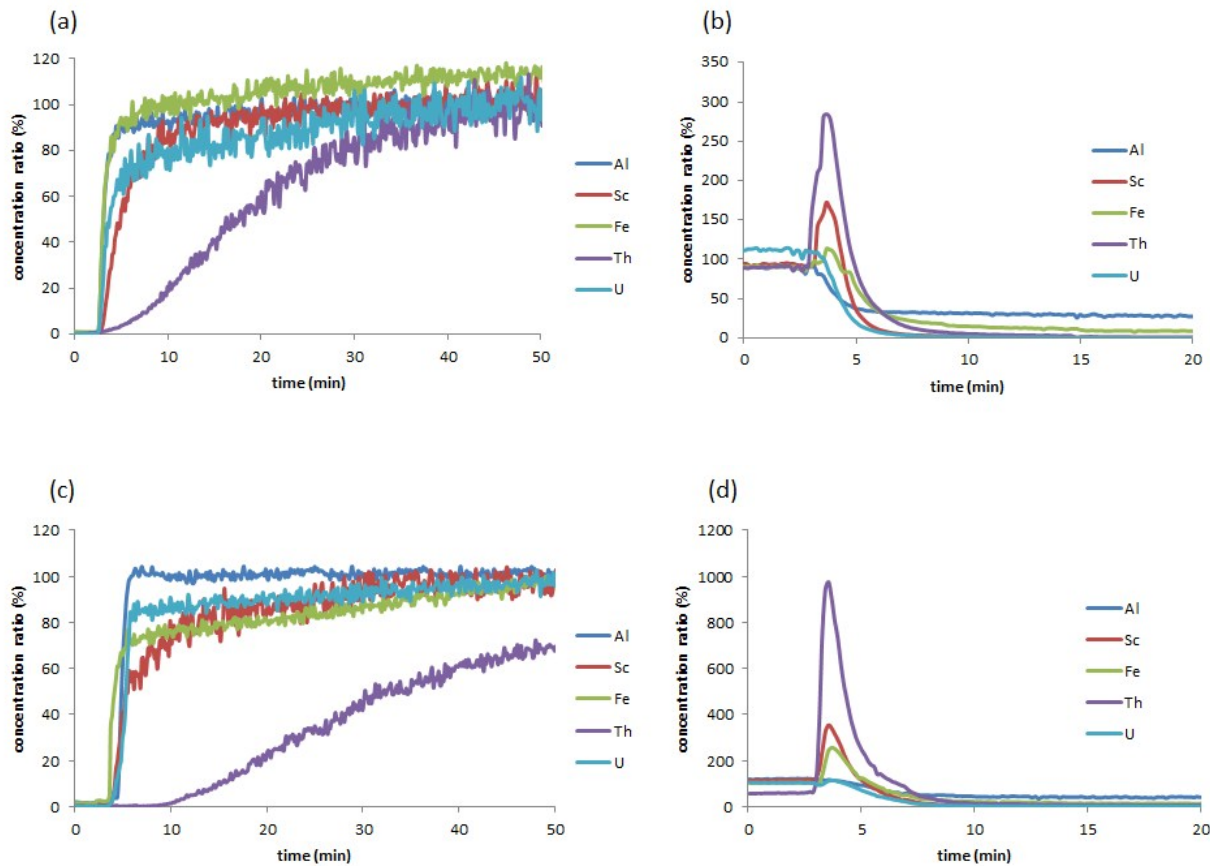


Figure S11. Extraction chromatograms of Al, Sc, Fe, Sc, Th, and U with passivated monoliths M2-TMDS (a) and M-DGA-TMDS (c), and the corresponding recovery chromatograms of using 0.05 M ammonium oxalate (b and d). The initial feed solution contains REEs, Al, Fe, Th, and U (concentration of 300 $\mu\text{g L}^{-1}$, pH 3.0). For clarity, only Al, Sc, Fe, Sc, Th, and U are shown here.

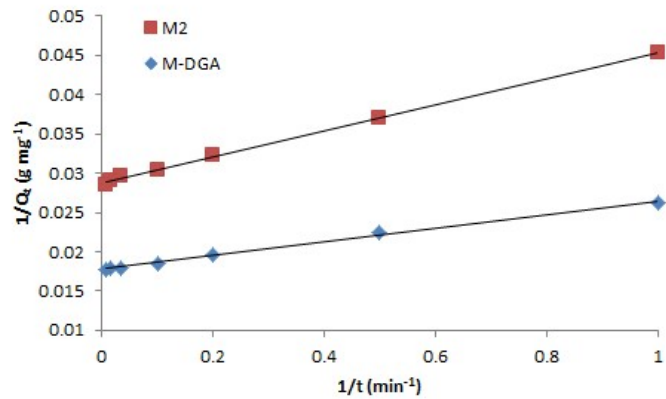


Figure S12. Linear regression of the pseudo-second-order kinetic model for adsorption of Th(IV) on M2 and M-DGA under batch extraction conditions.

The kinetic curves of M2 and M-DGA were fitted with pseudo-first-order (equation S1) and pseudo-second-order (equation S2) kinetic models as given below:

$$Q_t = Q_e - Q_e e^{-k_1 t} \quad (S1)$$

$$Q_t = \frac{k_2 Q_e^2 t}{1 + k_2 Q_e t} \quad (S2)$$

where Q_t (mg g^{-1}) and Q_e (mg g^{-1}) represent the amount of lutetium captured at time t , and at equilibrium, respectively; k_1 (L min^{-1}) and k_2 ($\text{g mg}^{-1} \text{ min}^{-1}$) are the rate constant of the pseudo-first-order and pseudo-second-order models. In addition, the half equilibrium time $t_{1/2}$ (min) of pseudo-second-order kinetic can be calculated according to equation S3:

$$t_{1/2} = \frac{1}{k_2 Q_e} \quad (S3)$$

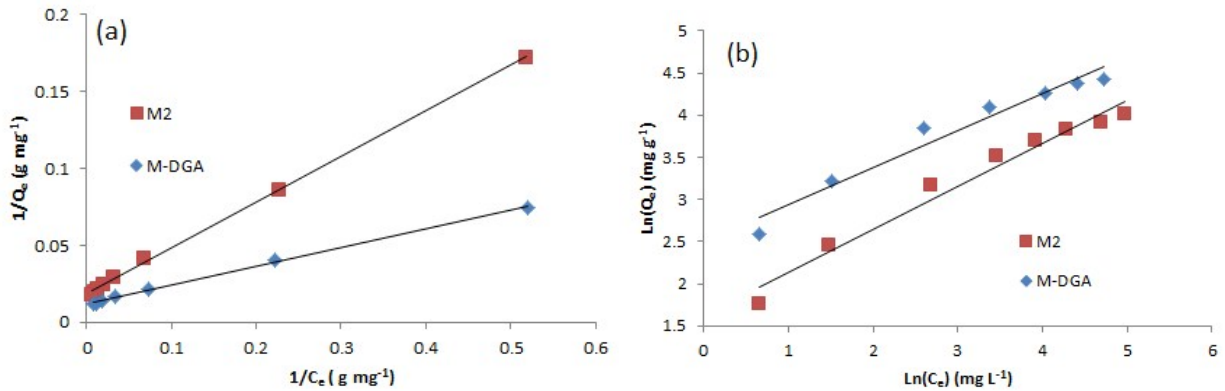


Figure S13. Linear regression of the Langmuir (a) and Freundlich (b) isotherm model of M2 and M-DGA used for the adsorption isotherms experiments.

The equations of the Langmuir (equation S4) and Freundlich (equation S5) isotherm models were expressed as follows:

$$Q_e = \frac{K_L Q_m C_e}{1 + K_L C_e} \quad (S4)$$

$$Q_e = K_F C_e^{1/n} \quad (S5)$$

where C_e (mg L⁻¹) stands for the equilibrium concentration, and Q_e (mg g⁻¹) is the adsorption capacity at equilibrium. Q_m (mg g⁻¹) represents the maximum adsorption capacity of the materials. K_L (L g⁻¹) is the affinity constant, and K_F (mg g⁻¹) represents the adsorption capacity direction constant, and $1/n$ indicates favorable adsorption condition.

For the Langmuir model, the separation factor (or equilibrium parameter constant) R_L can be obtained from the following equation S6:

$$R_L = \frac{1}{1 + C_m K_L} \quad (S6)$$

where C_m (mg g^{-1}) is the maximum initial concentration.

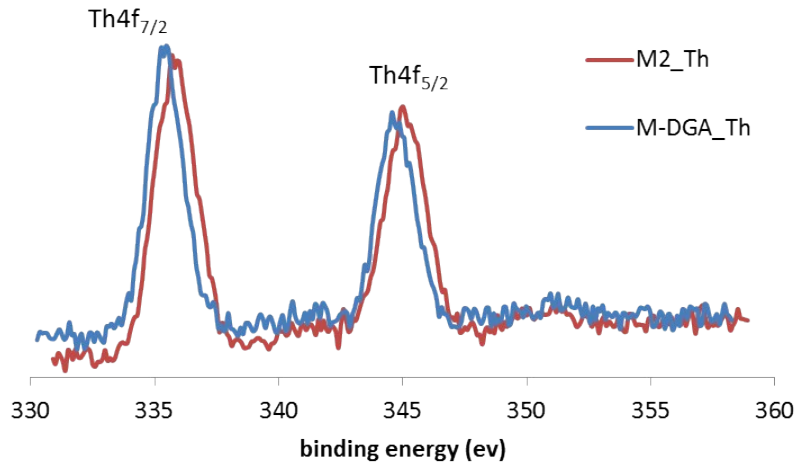


Figure S14. Th 4f XPS spectra of Th(IV)-loaded M2 and M-DGA.

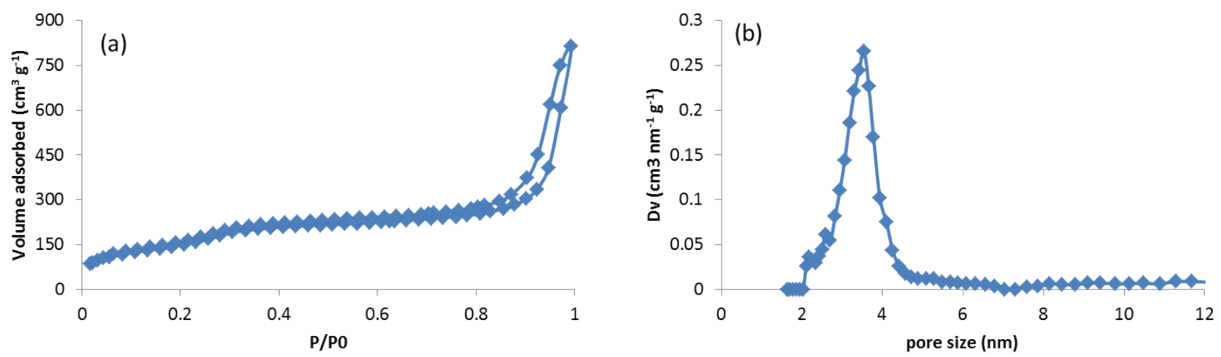


Figure S15. N₂ physisorption isotherm at -196 °C of M-DGA after the reusability test (a) and the corresponding NLDFT pore size distribution (b).

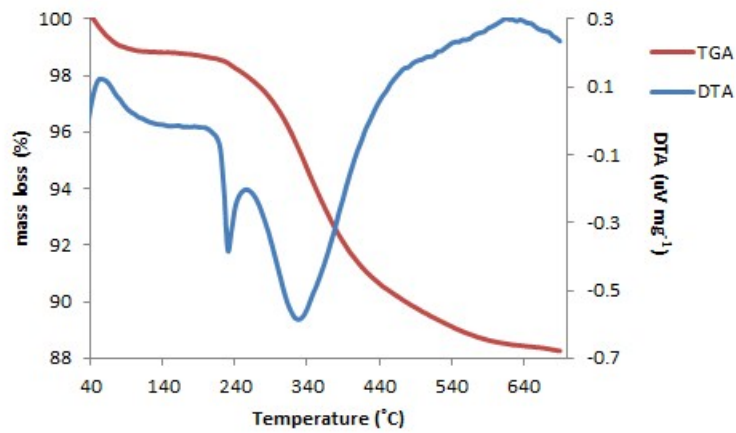


Figure S16. TGA and DTA curves of M-DGA after the reusability test.

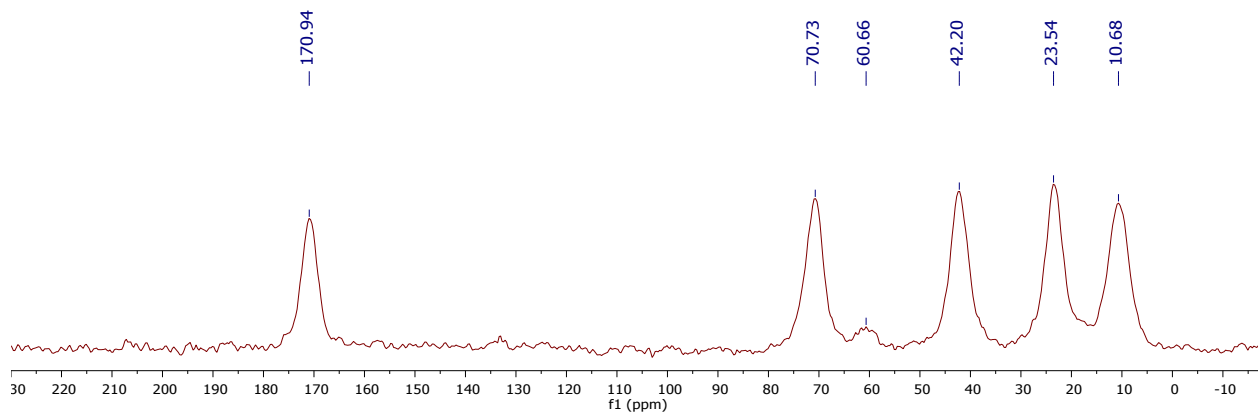


Figure S17. ^{13}C CP/MAS NMR spectrum of M-DGA after the reusability test.

Table S1. Synthesis conditions and physicochemical properties of the materials as measured by N₂ physisorption and mercury porosimetry.

	N ₂ physisorption measurement parameters			Hg porosimetry measurement parameters		Mass loss
samples	S _{BET} (m ² g ⁻¹)	Mesopore size (nm)	V _{mesopore} (cm ³ g ⁻¹)	Macropore size (μm)	V _{macropore} (cm ³ g ⁻¹)	TGA (%)
M0	693	2.6	0.35	1.2	1.11	-
M0.1	653	3.7	1.19	2.4	3.60	-
M0.5	641	3.8	1.21	4.3	3.98	-
M1	632	3.9	1.20	1.7	4.53	-
M2_75	626	4.0	1.17	2.7	3.86	-
M2-TMDS	610	3.8	1.60	-	-	2.9
M-DGA-TMDS	430	3.1	0.81	-	-	15.6
MCM-41	1410	4.0	1.25	-	-	-
MCM-41-DGA	896	3.2	0.56	-	-	20.1
KIT-6	935	8.5	1.25	-	-	-
KIT-6-DGA	642	7.2	0.89	-	-	25.8

Table S2. Kinetic constants for the pseudo-first-order and pseudo-second-order models.

Materials	Pseudo-first-order				Pseudo-second-order			
	$Q_{e,exp}$ (mg g ⁻¹)	$Q_{e,cal}$ (mg g ⁻¹)	k_1 (L min ⁻¹)	R^2	$Q_{e,cal}$ (mg g ⁻¹)	k_2 (g mg ⁻¹ min ⁻¹)	$t_{1/2}$ (min)	R^2
M2	35.0	33.3	0.97	0.98	34.7	0.050	0.57	0.99
M-DGA	56.1	53.4	0.59	0.93	55.6	0.036	0.49	0.99

Table S3. Adsorption equilibrium constants for Langmuir and Freundlich isotherm models.

Materials	Langmuir isotherm					Freundlich isotherm		
	$Q_{m,exp}$ (mg g ⁻¹)	$Q_{m,cal}$ (mg g ⁻¹)	K_L (L mg ⁻¹)	R_L	R^2	K_F (mg g ⁻¹)	$1/n$	R^2
M2	55.1	54.3	0.062	0.092	0.99	5.11	0.51	0.97
M-DGA	83.6	84.5	0.098	0.049	0.99	12.2	0.44	0.96

Table S4. Original elemental composition of OKA-2 and bauxite residue.

	OKA-2 (mg L ⁻¹)	Bauxite residue (mg L ⁻¹)
Sc	0.022	6.01
Y	499	2.15
La	7200	44.6
Ce	25 200	78.2
Pr	2790	8.55
Nd	12 410	29.1
Sm	2260	4.12
Eu	520	0.778
Gd	1760	3.40
Tb	180	0.322
Dy	460	1.05
Ho	46	0.138
Er	143	0.399
Tm	5.2	0.0340
Yb	36	0.205
Lu	5.4	0.0330
Th	159	26.1
U	116	1.58
Al	0.819	56632
Fe	22.3	868
Na	17	44918
Ca	71	14392
Si	43	50331

Ti	Not detected	2.59
----	--------------	------

Table S5. Extraction percentages of M-DGA for OKA-2 and bauxite residue solutions.

	OKA-2 (%)	Bauxite residue (%)
Sc	65.83	31.76
Y	0.033	2.16
La	0.019	1.12
Ce	0.012	0.138
Pr	0.322	2.64
Nd	0.103	1.97
Sm	0.010	4.45
Eu	0.011	1.5397
Gd	0.010	4.774762
Tb	0.045	3.116791
Dy	0.043	2.152755
Ho	0.419	0.29022
Er	0.048	3.73
Tm	0.047	6.54175
Yb	0.592	0.4197
Lu	0.642	6.16
Th	95.48	81.39
U	2.67	1.54
Al	63.24	3.814
Fe	54.27	27.89
Na	0.038	0.802
Ca	0.482	0.017

Si	0	0
----	---	---